

Theory of vortex excitation imaging via an NMR relaxation measurement

Mitsuaki Takigawa, Masanori Ichioka and Kazushige Machida
Department of Physics, Okayama University, Okayama 700-8530, Japan
(October 9, 2018)

The temperature dependence of the site-dependent nuclear spin relaxation time T_1 around vortices is studied in *s*-wave and *d*-wave superconductors. Reflecting low energy electronic excitations associated with the vortex core, temperature dependences deviate from those of the zero-field case, and T_1 becomes faster with approaching the vortex core. In the core region, T_1^{-1} has a new peak below T_c . The NMR study by the resonance field dependence may be a new method to prove the spatial resolved vortex core structure in various superconductors.

PACS numbers: 74.60.Ec, 74.25.Jb, 76.60.Pc

Much attention has been focused on vortex physics both of high T_c cuprates and of conventional superconductors. Among various experimental methods, the nuclear magnetic resonance (NMR) experiments¹ have been providing vital data in distinguishing between *s*-wave and *d*-wave pairing symmetries via temperature (T) dependence of the nuclear spin relaxation time T_1 , which reflects low-lying excitations in the superconducting state. The power law $T_1^{-1} \propto T^3 (T^5)$ behavior is taken as definitive evidence for a line (point) node in the gap structure of anisotropic superconductors. This conclusion comes from a simple counting of the density of states (DOS) at the Fermi level: $N(\omega) \propto \omega (\omega^3)$ for a line (point) node in a bulk superconductor at zero field. However, actual NMR experiments are performed under applied fields in a mixed state. Then, the contribution of the vortex core is included in their data^{2,3}. Usually, T_1 is measured by selecting the resonance frequency at a most intensive signal in the resonance spectrum. However, the resonance spectrum reflects information of internal magnetic field distribution of the vortex lattice⁴. By choosing the resonance field, we can specify the position to detect the NMR signal. The signal at the maximum (minimum) cutoff comes from the vortex center (the furthest) site. The signal at the logarithmic singularity of the resonance field comes from the saddle points of the field. By studying the position dependence of T_1 around vortices through the resonance frequency dependence, we can clarify the detail of the vortex contribution in the NMR experiments. It helps us in the analysis of the standardized procedure extracting the gap symmetry.

Low-lying excitation spectra around a vortex are not fully understood both experimentally and theoretically. The related problems are as follows. In the *s*-wave superconductors, the effect of the quantized energy level will appear in the quasi-particle state⁵⁻⁷. In the *d*-wave case, the low energy state around the vortex core extends outside the core due to the node of the superconducting gap, and shows the \sqrt{H} -like DOS relation (H is an applied field)⁸⁻¹². We also need to estimate the quasi-particle transfer between vortices (such as the path of the transfer and its amplitude) to study the dHvA oscillation or transport phenomena in the mixed state^{9,13}.

The excitation around the core plays a fundamental role in determining physical properties of superconductors. In high T_c cuprates, the existence or non-existence of localized core excitations in *d*-wave pairing case is actively debated. Theoretical study suggested the zero-energy peak in the *d*-wave case, instead of the quantized energy level in the *s*-wave case¹⁰⁻¹². On the contrary, the scanning tunneling spectroscopy (STS) experiments reported quantized energy level with large gap in YBCO¹⁴, and surprisingly enough no peak within the superconducting gap in BSCCO¹⁵. A part of reasons of the debate is due to limited experimental methods which directly probe the spatially resolved core structure. So far, the STS was only a method to detect it. A large number of thermodynamic or transport measurements probe spatially averaged quantities. Here we propose a novel spatially resolved means, that is, vortex imaging to see electronic excitations associated with a vortex core by using NMR, and demonstrate how the T -dependence of T_1 is site-sensitive. Through this analysis, we are able to produce a spatial image of the low-lying excitation spectrum around a core. A similar idea of the NMR imaging is actually tested experimentally in high T_c materials by Slichter's group¹⁶ and also in spin-Peierls system CuGeO₃ by Horvatić¹⁷.

The position dependence of the NMR signal in the *s*-wave case was theoretically studied under some approximations^{6,18}. Here, we calculate it microscopically from the wave functions obtained by self-consistently solving the Bogoliubov-de Gennes (BdG) equation for the extended Hubbard model in the *s*- and *d*-wave cases. The eigen-energy E_α and the wave functions $u_\alpha(\mathbf{r}_i)$, $v_\alpha(\mathbf{r}_i)$ at i -site are calculated by following the method of Ref. 11. The BdG equation for the extended Hubbard model on the two-dimensional square lattice is given by

$$\sum_j \begin{pmatrix} K_{i,j} & D_{i,j} \\ D_{i,j}^* & -K_{i,j}^* \end{pmatrix} \begin{pmatrix} u_\alpha(\mathbf{r}_j) \\ v_\alpha(\mathbf{r}_j) \end{pmatrix} = E_\alpha \begin{pmatrix} u_\alpha(\mathbf{r}_i) \\ v_\alpha(\mathbf{r}_i) \end{pmatrix}, \quad (1)$$

where $K_{i,j} = -t_{i,j} \exp[i \frac{\pi}{\phi_0} \int_{\mathbf{r}_i}^{\mathbf{r}_j} \mathbf{A}(\mathbf{r}) \cdot d\mathbf{r}] - \delta_{i,j} \mu$, $D_{i,j} = \delta_{i,j} U \Delta_{i,i} + \frac{1}{2} V_{i,j} \Delta_{i,j}$ with the on-site interaction U , the chemical potential μ and the flux quantum ϕ_0 . The transfer integral $t_{i,j} = t$ and the nearest neighbor(NN) interac-

tion $V_{i,j} = V$ for the NN site pair \mathbf{r}_i and \mathbf{r}_j , and otherwise $t_{i,j} = V_{i,j} = 0$. The vector potential $\mathbf{A}(\mathbf{r}) = \frac{1}{2}\mathbf{H} \times \mathbf{r}$ in the symmetric gauge. The self-consistent condition for the pair potential is

$$\Delta_{i,j} = -\frac{1}{2} \sum_{\alpha} u_{\alpha}(\mathbf{r}_i) v_{\alpha}^*(\mathbf{r}_j) \tanh(E_{\alpha}/2T). \quad (2)$$

The band filling factor $\langle n \rangle \sim 0.9$ in our calculation.

We consider the square vortex lattice case where nearest neighbor vortex is located at the 45° direction from the a axis. This vortex lattice configuration is suggested for d -wave superconductors, or s -wave superconductors with fourfold symmetric Fermi surface^{9,19,20}. The unit cell in our calculation is the square area of N_r^2 sites where two vortices are included. Then, $H = 2\phi_0/(cN_r)^2$ (c is the atomic lattice constant). We consider the area of N_k^2 unit cells. By introducing the quasi-momentum of the magnetic Bloch state, $\mathbf{k} = (2\pi/cN_rN_k)(l_x, l_y)$ ($l_x, l_y = 1, \dots, N_k$), we set $u_{\alpha}(\mathbf{r}) = \tilde{u}_{\alpha}(\mathbf{r})e^{i\mathbf{k} \cdot \mathbf{r}}$, $v_{\alpha}(\mathbf{r}) = \tilde{v}_{\alpha}(\mathbf{r})e^{i\mathbf{k} \cdot \mathbf{r}}$. We solve Eq. (1) within a unit cell under the given \mathbf{k} . Then, α is labeled by \mathbf{k} and the eigen-values obtained by this calculation within a unit cell.

The periodic boundary condition is given by the symmetry for the translation $\mathbf{R} = m\mathbf{u}_1 + n\mathbf{u}_2$ (m and n are integers, \mathbf{u}_1 and \mathbf{u}_2 are unit vectors of the vortex lattice), i.e., $\tilde{u}_{\alpha}(\mathbf{r} + \mathbf{R}) = \tilde{u}_{\alpha}(\mathbf{r})e^{i\chi(\mathbf{r}, \mathbf{R})/2}$, $\tilde{v}_{\alpha}(\mathbf{r} + \mathbf{R}) = \tilde{v}_{\alpha}(\mathbf{r})e^{-i\chi(\mathbf{r}, \mathbf{R})/2}$. Here, $\chi(\mathbf{r}, \mathbf{R}) = -\frac{2\pi}{\phi_0} \mathbf{A}(\mathbf{r}) \cdot \mathbf{R} - \pi mn + \frac{2\pi}{\phi_0} (\mathbf{H} \times \mathbf{r}_0) \cdot \mathbf{R}$ in the symmetric gauge when the vortex center is located at $\mathbf{r}_0 + \frac{1}{2}(\mathbf{u}_1 + \mathbf{u}_2)$. The on-site s -wave pair potential $\Delta_s(\mathbf{r}_i) = U\Delta_{i,i}$. The $d_{x^2-y^2}$ -wave pair potential is given by

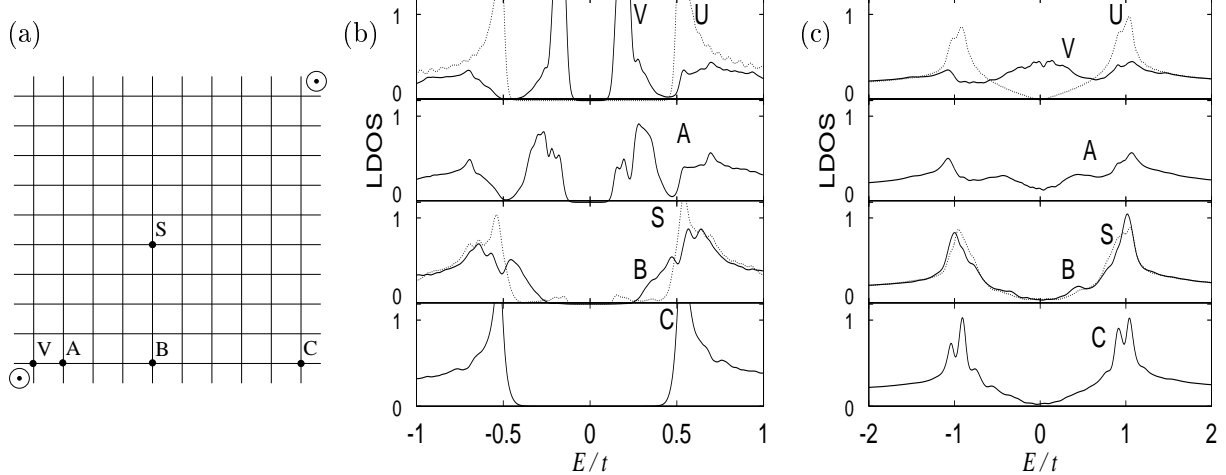


FIG. 1. The LDOS $N(\mathbf{r}, E)$ at sites V, A, B, C, S. (a) Position of the sites V, A, B, C, S in the square vortex lattice, where the nearest neighbor vortex is located in the 45° direction from the a -axis. The vortex center is shown by \odot . The solid lines show the square atomic lattice. (b) $N(\mathbf{r}, E)$ in the s -wave case. (c) $N(\mathbf{r}, E)$ in the d -wave case. The LDOS for the S-site is presented by the dotted line with the solid line for the B-site. The DOS at zero-field is presented by the dotted line U with the solid line for the V-site.

$$\Delta_d(\mathbf{r}_i) = V(\Delta_{\hat{x},i} + \Delta_{-\hat{x},i} - \Delta_{\hat{y},i} - \Delta_{-\hat{y},i})/4 \quad (3)$$

with $\Delta_{\pm\hat{e},i} = \Delta_{i,i\pm\hat{e}} \exp[i\frac{\pi}{\phi_0} \int_{\mathbf{r}_i}^{(\mathbf{r}_i+\mathbf{r}_{i\pm\hat{e}})/2} \mathbf{A}(\mathbf{r}) \cdot d\mathbf{r}]$. The phase factor²¹ is needed to satisfy the translational relation $\Delta_d(\mathbf{r}) = \Delta_d(\mathbf{r} + \mathbf{R})e^{i\chi(\mathbf{r}, \mathbf{R})}$.

We construct the Green's functions from E_{α} , $u_{\alpha}(\mathbf{r})$, $v_{\alpha}(\mathbf{r})$, and calculate the spin-spin correlation function $\chi_{+-}(\mathbf{r}, \mathbf{r}', i\Omega_n)^{18}$. Then, we obtain the nuclear spin relaxation rate,

$$\begin{aligned} R(\mathbf{r}, \mathbf{r}') &= \text{Im} \chi_{+-}(\mathbf{r}, \mathbf{r}', i\Omega_n \rightarrow \Omega + i\eta) / (\Omega/T)|_{\Omega \rightarrow 0} \\ &= - \sum_{\alpha, \alpha'} u_{\alpha}(\mathbf{r}) u_{\alpha'}^*(\mathbf{r}) [u_{\alpha}(\mathbf{r}') u_{\alpha'}^*(\mathbf{r}') + v_{\alpha}(\mathbf{r}') v_{\alpha'}^*(\mathbf{r}')] \\ &\quad \times \pi T f'(E_{\alpha}) \delta(E_{\alpha} - E_{\alpha'}) \end{aligned} \quad (4)$$

with the Fermi distribution function $f(E)$. We consider the case $\mathbf{r} = \mathbf{r}'$ by assuming that the nuclear relaxation occurs locally such as in Cu-site of high T_c cuprates. Then, \mathbf{r} -dependent relaxation time is given by $T_1(\mathbf{r}) = 1/R(\mathbf{r}, \mathbf{r})$. In Eq. (4), we use $\delta(x) = \pi^{-1} \text{Im}(x - i\eta)^{-1}$ to consider the discrete energy level of the finite size calculation. We typically use $\eta = 0.01t$. To understand the behavior of $T_1(\mathbf{r})$, we also consider the local density of states (LDOS) given by

$$\begin{aligned} N(\mathbf{r}, E) &= - \sum_{\alpha} [|u_{\alpha}(\mathbf{r})|^2 f'(E_{\alpha} - E) + |v_{\alpha}(\mathbf{r})|^2 f'(E_{\alpha} + E)]. \end{aligned} \quad (5)$$

It corresponds to the differential tunnel conductance of STS experiments.

As for the temperature dependence of $\Delta_s(\mathbf{r})$ and $\Delta_d(\mathbf{r})$, the vortex core radius shrinks with decreasing T by the Kramer-Pesch effect^{10,22}. However the shrink is saturated at a low temperature both in the s - and d -wave cases. There, the structure of $\Delta_s(\mathbf{r})$ and $\Delta_d(\mathbf{r})$ is almost independent of T . This is a quantum-limit effect which occurs for $T/T_c < \Delta_0/E_F$ (E_F is the Fermi energy and Δ_0 the superconducting gap at zero field). In our calculation, $\Delta_0/E_F \sim 0.25$ for d -wave, ~ 0.125 for s -wave)⁷. We calculate the low temperature behavior of $T_1(\mathbf{r})$ by using the saturated pair potential. At higher temperature, we calculate $T_1(\mathbf{r})$ by using the self-consistently obtained pair potential at each T .

Figure 1 (a) shows the position of the sites (V, A, B, C, S) where we calculate $N(E, \mathbf{r})$ and $T_1(\mathbf{r})$. First, we see the LDOS around the vortex. The s -wave case ($U = -2.32t$, $V = 0$) is shown in Fig. 1(b), and the d -wave case ($U = 0$, $V = -4.20t$) is shown in Fig. 1(c). In our calculation, $N_r = 20$ and $N_k = 8$. In $N(E, \mathbf{r})$ at the vortex center (the V-site), the gap edge at Δ_0 in the zero-field case (dotted line U) is smeared, and low-energy peaks of the vortex core state appear. In the s -wave case, we see some peaks above the small gap Δ_1 ($\sim \Delta_0^2/E_F$). It is due to the quantization of the energy level in the s -wave case. In the d -wave case, the core state shows zero-energy peak instead of the split peaks in the s -wave case¹¹. There is no small gap. The weight of the low-energy states is decreased with going away from the vortex center (V \rightarrow A \rightarrow B \rightarrow C). Far from the vortex, $N(E, \mathbf{r})$ is reduced to the DOS of the zero-field case. But, small weight of the low-energy state extending from the vortex core remains there. It is noted that the weight of the low-energy state at the S-site is larger than that of the B-site in the s -wave case, while the S-site is farther from the vortex center [see lines for the S- and B-sites in Fig 1(b)]. It is due to the vortex lattice effect. The quasi-particle transfer between vortices occurs along the line connecting NN vortices (i.e., near the S-site).

Next, we consider the T -dependence of $T_1(\mathbf{r})$ at each site in Fig. 1, which reflects the LDOS discussed above. The NMR signal at the maximum cutoff of the resonance spectrum as a function of applied field or probe frequency comes from the vortex core at the V-site. With going away from the center (V \rightarrow A \rightarrow B \rightarrow C), the resonance field is decreased. The signal at the minimum cutoff comes from the C-site. The logarithmic singularity of the resonance field comes from the saddle point of the field at the S-site. Thus it is possible to perform the site-selective $T_1(\mathbf{r})$ measurement by tuning the resonance frequency.

The s -wave case is shown in Fig. 2. We plot $T_1(\mathbf{r})^{-1}$ vs. T for each site in Fig. 2(a), and re-plot it as $\ln T_1(\mathbf{r})$ vs. T^{-1} in Fig. 2(b). We also calculate the zero-field case in our formulation. At the zero field, $T_1 \sim e^{\Delta_0/T}$. Then, the slope of the $\ln T_1$ vs. T^{-1} plot gives the superconducting gap Δ_0 , as the line U in Fig. 2(b). In the presence of vortices, T_1 deviates from the relation $e^{\Delta_0/T}$ at low T due to the low-energy excitation around the vortex core. This deviation was reported in the experi-

ments². In our results, reflecting the small gap Δ_1 in the s -wave case, T_1 shows the slope Δ_1 at low T in the $\ln T_1$ vs. T^{-1} plot (see the V-site in Fig. 1(b)) as seen in Fig. 2(b). That is, $T_1 \sim e^{\Delta_1/T}$. With leaving the vortex center, since the amplitude of the low-energy bound states is damped, the weight of $e^{\Delta_1/T}$ gradually decreases. Then the crossover temperature from $e^{\Delta_0/T}$ to $e^{\Delta_1/T}$ is lowered. It is noted that T_1 is faster at the S-site than that of the B-site, while the S-site is further from the vortex center. This non-trivial result is due to the vortex lattice effect noted above. We should also notice the behavior of the coherence peak below T_c . As seen in Fig. 2(a), with approaching the vortex center as C \rightarrow B, the coherence peak is suppressed. But in the vortex core region (lines V and A), a large new peak grows at intermediate temperatures. This is because the LDOS at the vortex core has peaks at low energy Δ_1 instead of the singularity of DOS at Δ_0 .

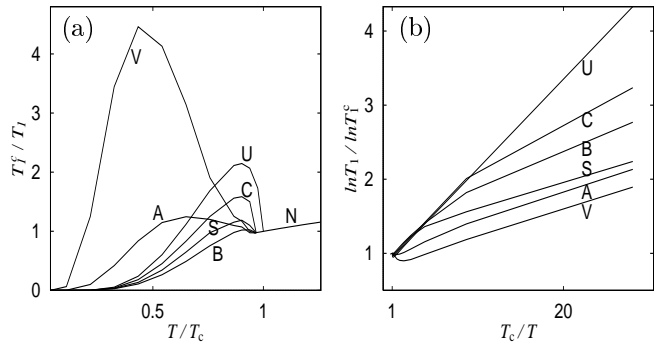


FIG. 2. Temperature dependence of $T_1(\mathbf{r})$ in the s -wave case at the sites V, A, B, C, S assigned in Fig. 1(a). (a) $T_1(T_c)/T_1(T)$ is plotted as a function of T/T_c . (b) $\ln T_1(T)/\ln T_1(T_c)$ is plotted as a function of T_c/T . Line U shows the zero field case. The line N is for the normal state at $T > T_c$.

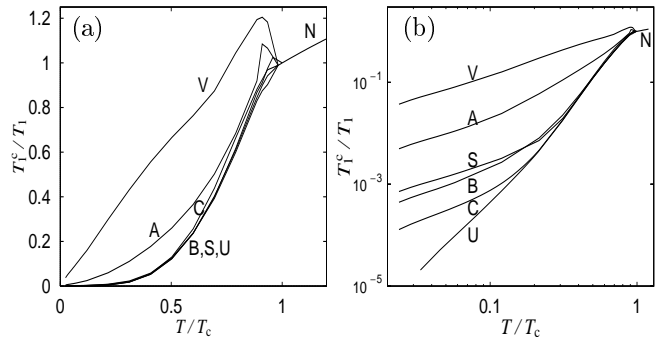


FIG. 3. Temperature dependence of $T_1(\mathbf{r})$ in the d -wave case at the sites V, A, B, C, S. (a) $T_1(T_c)/T_1(T)$ is plotted as a function of T/T_c . (b) a log-log plot of (a). Line U shows the zero field case. The line N is for the normal state at $T > T_c$.

As for the d -wave case, we plot $T_1(\mathbf{r})^{-1}$ vs. T in Fig. 3(a), and re-plot it as a log-log plot in Fig. 3(b). At zero field (line U), we see the power law relation $T_1^{-1} \sim T^3$ of the d -wave case as expected. Note that this can be seen only below $T/T_c \simeq 0.1$ in our case. In the presence of vortices, $T_1(\mathbf{r})^{-1}$ deviates from the T^3 -relation, and follows $T_1(\mathbf{r})^{-1} \sim T$ at low temperature. This deviation was reported in the experiments on high- T_c cuprates³. The origin of the T -linear behavior, which is attributed to residual density of states due to impurities or defects, is the low-energy state around vortices in our case. With approaching the vortex center, the T region of the T -linear behavior is enlarged and it appears from higher temperatures. As seen in Fig. 1(c) of the d -wave case, the superconducting gap is buried by the low-energy state around vortices without the small gap of the order Δ_0^2/E_F . Then, $T_1^{-1} \sim T$ at low temperature in the d -wave case instead of the relation $T_1 \sim e^{\Delta_1/T}$ in the s -wave case. As seen in Fig. 3, $T_1(\mathbf{r})^{-1}$ at the vortex center (line V) is very large compared with the zero-field case (line U). It reflects the fact that the LDOS of the low-energy state is larger than the DOS of the zero-field case as seen in Fig. 1(c). This short relaxation may be the evidence of the low-energy peak in the LDOS by the low-energy core state. The coherence peak below T_c is taken as a manifestation of the s -wave symmetry. In the d -wave case, the coherence peak is absent. But in the vortex core region, T_1^{-1} has a peak below T_c even in the d -wave case. We should be careful not to mistake this peak due to the vortex core relaxation as the usual coherence peak in the NMR experiment when identifying the gap symmetry.

With increasing external magnetic field, the relaxation is enhanced, because the vortex contribution is increased and the amplitude of the low energy state extending outside the vortex core becomes large both in the s -wave and d -wave cases, as coinciding qualitatively with the observation of an organic superconductor κ -(ET)₂Cu[N(CN)₂]Br by Mayaffre *et al.*²³. The details of the field dependence belong to a future study.

Traditionally, the vortex contribution was considered as the spin diffusion to the normal region of the vortex core^{3,6}, and T_1 is treated as the spatial average. However, we can investigate the position dependence of $T_1(\mathbf{r})$ around vortices through the resonance field dependence. This is an advantage of NMR over other methods. We should clarify the local mechanism of the relaxation (i.e., whether the relaxation occurs locally, or it is averaged by the spin diffusion). It is noted that in the clean limit the vortex core region is not a simple core filled by normal state electrons⁹. There, the characteristic T -dependence is expected near the vortex core other than a simple T -linear behavior, reflecting the rich structure of the low energy state around the vortex core. We expect that the NMR imaging study just explained here will provide vital information for the vortex core state in high- T_c cuprates. As for the problem whether the quantization of the energy levels occurs or not, $T_1 \sim e^{\Delta_1/T}$ if the gap Δ_1

($\sim \Delta_0^2/E_F$) is present in the excitation due to the quantization. If this small gap is absent, $T_1^{-1} \sim T$. As for the problem whether the zero-energy peak exists or not in the core state, the relaxation at the core becomes eminently faster than that of the zero-field case (or that far from the vortex) at low temperature, if the zero-energy peak exists in the LDOS as suggested in the theoretical study. If the peak structure is absent within Δ_0 as reported in the STM experiments on BSCCO, the relaxation is slow even at the vortex core as in the zero-field superconducting case.

We proposed the study of the low-energy excitation imaging around vortices via an NMR relaxation. It may provide valuable information for the understanding of the vortex physics in high- T_c superconductors as well as in the conventional superconductors.

We thank M. Horvatić, K. Ishida and Y. Iwamoto for useful information on NMR experiments.

¹ See for example, recent technical developments: J. Haase, N.J. Curro, R. Stern, and C.P. Slichter, Phys. Rev. Lett. **81**, 1489 (1998). K.R. Gorny, O.M. Vyaselev, S. Yu, C.H. Pennington, W.L. Hults, and J.L. Smith, *ibid* 2340.

² B.G. Silbernagel, M. Weger, and J.E. Wernick, Phys. Rev. Lett. **17**, 384 (1966).

³ K. Ishida, Y. Kitaoka, and K. Asayama, Solid State Commun. **90**, 563 (1994). K. Ishida, Y. Kitaoka, K. Asayama, K. Kadowaki, and T. Mochiku, J. Phys. Soc. Jpn. **63**, 1104 (1994).

⁴ W. Fite, II and A.G. Redfield, Phys. Rev. Lett. **17**, 381 (1966).

⁵ C. Caroli, P.-G. de Gennes, and J. Matricon, Phys. Lett. **9**, 307 (1964).

⁶ C. Caroli and J. Matricon, Phys. Kondens. Mater. **3**, 380 (1965).

⁷ N. Hayashi, T. Isoshima, M. Ichioka, and K. Machida, Phys. Rev. Lett. **80** 2921 (1998).

⁸ G. E. Volovik, JETP Lett. **58**, 469 (1993).

⁹ M. Ichioka, A. Hasegawa, and K. Machida, Phys. Rev. B **59**, 184, 8902 (1999).

¹⁰ M. Ichioka, N. Hayashi, N. Enomoto, and K. Machida, Phys. Rev. B **53**, 15316 (1996).

¹¹ Y. Wang and A.H. MacDonald, Phys. Rev. B **52**, 3876 (1995).

¹² M. Franz and Z. Tešanović, Phys. Rev. Lett. **80**, 4763 (1998).

¹³ M. Ichioka, N. Hayashi, and K. Machida, Phys. Rev. B **55**, 6565 (1997).

¹⁴ I. Maggio-Aprile, Ch. Renner, A. Erb, E. Walker, and Ø. Fischer, Phys. Rev. Lett. **75**, 2754 (1995); J. Low Temp. Phys. **105**, 1129 (1996).

¹⁵ Ch. Renner, B. Revaz, K. Kadowaki, I. Maggio-Aprile, and Ø. Fischer, Phys. Rev. Lett. **80**, 3606 (1998).

¹⁶ N.J. Curro, C.P. Slichter, W.C. Lee, and D.M. Ginsberg,

A.P.S. March Meeting Abstract (1999).

¹⁷ M. Horvatić, private communication.

¹⁸ R. Leadon and H. Suhl, Phys. Rev. **165**, 596 (1968).

¹⁹ *The superconducting state in magnetic fields* edited by C.A.R. Sá de Melo, (world scientific, Singapore, 1998), Chaps. 7 and 8.

²⁰ H. Won and K. Maki, Phys. Rev. B **53**, 5927 (1996).

²¹ Our definition gives the same phase factor as that of M. Ozaki, Y. Hori, and A. Goto, Prog. Theor. Phys. **101**, 769 (1999).

²² L. Kramer and W. Pesch, Z. Phys. **269**, 59 (1974). W. Pesch and L. Kramer, J. Low Temp. Phys. **15**, 367 (1974).

²³ H. Mayaffre, P. Wzietek, D. Jérôme, C. Lenoir, and P. Batail, Phys. Rev. Lett. **75**, 4122 (1995).